

**Military Technical College  
Kobry El-Kobbah,  
Cairo, Egypt.**



**15<sup>th</sup> International Conference  
on Applied Mechanics and  
Mechanical Engineering.**

## **COMPUTATIONAL FLUID DYNAMIC ANALYSIS OF A THREE DIMENSIONAL LASER SCANNED PROPELLER USING CFX**

M.M. Shaheen\*, O. E. abdel-Hamid\*, M. A. El-Latif\* and W. A. Waba\*

### **ABSTRACT**

Conventional techniques used for measuring propellers geometric parameters are either destructive or in accurate or even time consuming. The outer surface of a two-Bladed wooden propeller of a powered Para-Parachute was scanned using a three dimensional laser scanner. A cloud of points has resulted out of the scanning process. Sections were taken in the cloud of points to draw the airfoil profiles at certain radii stations of the propeller, and then they were used to build a CAD model using CFX blade generator.

Before manufacturing a prototype a computational fluid dynamic analysis has been performed using CFX blade Gen+ in order to validate the measured data, the analysis of the inflow and outflow properties were used to calculate the thrust of the propeller showing results that satisfies the propeller available data. A prototype has been manufactured depending on the geometrical data obtained by laser scanning and a flight test has been performed where the propeller succeeded to generate the thrust required by the Powered Propeller to take off with its payload.

### **KEY WORDS**

Powered Para-gliders, three dimensional Laser scanner, CFX blade generator.

---

\* Egyptian Armed Forces.

## INTRODUCTION

Most of the Para-gliders are powered by wooden propellers for reasons of safety of the paratrooper in case of propeller destruction.



**Fig. 1.** Powered Para-glider.

Sandy terrain operation conditions and suction of small stones cause pitting in the leading edge of the wooden propeller changing its aerodynamic characteristics, and serious cracks in the propeller surface which propagate due to dynamic loading as shown in figure (2), causing fatigue failure of the propeller.

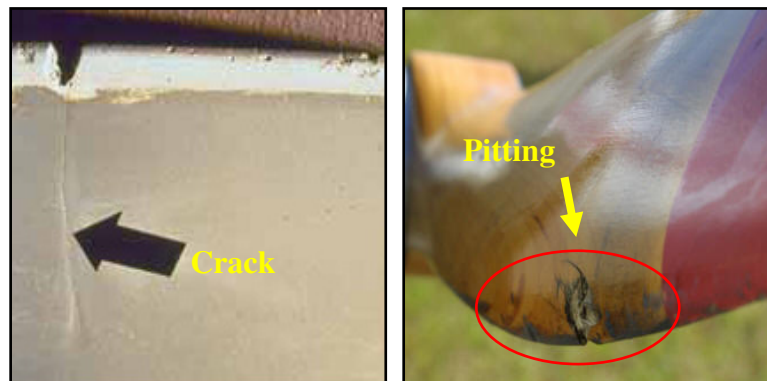


**Fig. 2.** Cracks and pitting on propeller blade surface.

Reverse engineering of propellers is a tough job; more particularly a propeller blade has a complex shape that requires identifying its geometric parameters (2D blade sections profiles, thickness distribution and pitch distribution) using a suitable measuring technique.

Creating of 2D drawing and 3D model for the propeller blade surface will be performed making use of the measured data in order to build a CFD model and analyze it in addition to manufacturing of templates used for the manufacturing process.

## PROPELLER MEASURING TECHNIQUES

Conventional techniques [1] used for measuring propellers geometric parameters shown in Fig. 3.

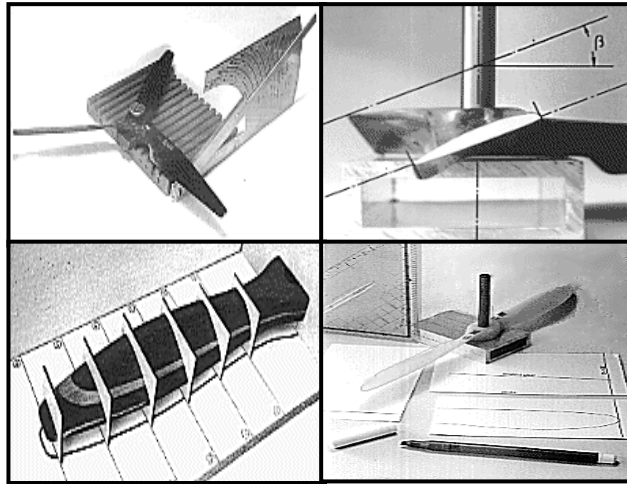


**Fig. 3.** Conventional propeller measuring techniques.

The development in the applications of Laser technology created a new generation of 3D scanners capable of measuring the geometry of complex shapes like propeller blades. The surface exposing to a Laser strip is interpreted as the a cloud of points, Passing by several qualification processes and modeling phases, starting from point phase to polygon phase to shape phase, a solid model can be created out of the cloud of points.

### Creating 2D and 3D Blade Surfaces and Propeller Design Data

In order to acquire propeller design data from the measured propeller geometric parameters, 2D and 3D blade surfaces has to be generated. General-case CAD software traditionally uses cylindrical coordinate system, the problem is that propellers do not easily conform to linear XYZ space, they rotate and advance along an axis and their natural coordinate system is helical [2-3].

Importing the geometric data and design constraints of the propeller blade to software specified in blade generation (CFX blade Gen) can be used to develop the blade surfaces and the propeller design data.

CFX blade Gen. develops a full 3D definition of the hydrodynamic blade surfaces and can package this data for export to conventional CAD, CAM and modeling software [4-5].

### Three Dimensional Laser Scanning of the Propeller Blade

The propeller blades are symmetric; only one blade with its hub was scanned for time saving. The propeller polished shiny surface scatters and diffuses Laser rays, so the propeller blade being scanned was painted white as shown in Fig.4.

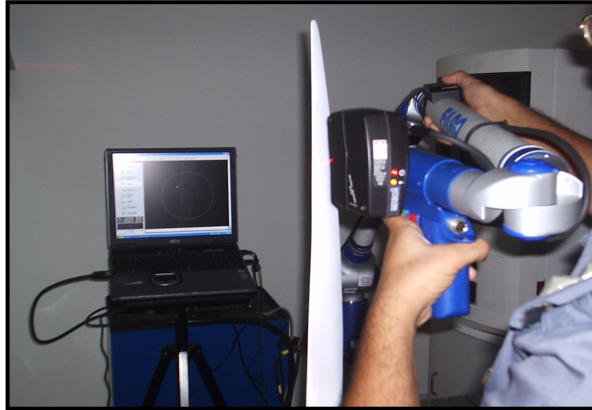


**Fig. 4.** Three dimensional Laser scanning of the propeller blade.

The scanning process was performed taking successive adjacent scanning shots until covering the whole surface of the propeller. The reflected Laser rays are captured by a laser sensor and the received data is interpreted as coordinates for each point on the scanned surface which appears as a cloud of points on the software accompanying the scanner system as shown in Fig.5.

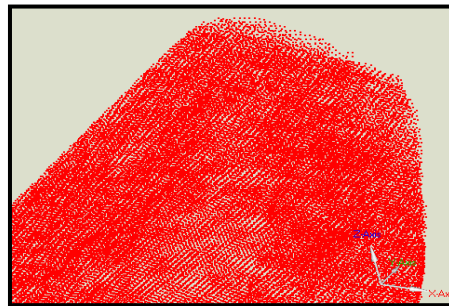


**Fig. 5.** Propeller cloud of points.

### **Creating Two Dimensional Sectional Profiles of the Propeller Blade**

A Blade Radius Station is a reference plane located at right angle to the blade center line at some distance out from the propeller center line towards the propeller tip. The adopted technique to create sectional profiles recommends the following radii stations: 0, 25, 40, 50, 60, 70, 80, 90, 100 percent radii stations [6] in order to provide an adequate number of points for contour checking during the blade carving operation, without involving excessive layout effort.

The cloud of points generated out of the scanning process was sliced at the several radii stations, using cutting planes parallel to the hub plane of symmetry and as shown in fig.6. , then the recommended radii stations were selected as work stations, and exported as a DXF file, where they were cleaned and modified in AutoCAD.

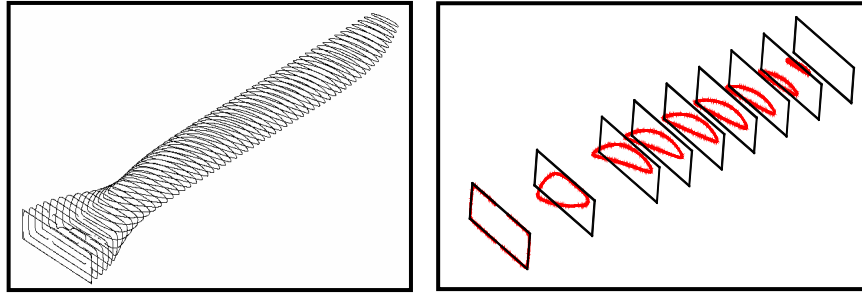


**Fig. 6.** Sectioning the cloud of points.

### THREE DIMENSIONAL MODELING OF PROPELLER USING CFX BLADE GEN.

#### Defining Sectional Meridional Data

To define the profile of an airfoil, the coordinates of points of its meridional in addition to the normal thickness at these points had to be defined and this was done for each recommended radius station as follows:

Drawing a copy of the hub rectangular cross section at each radius station, and taking the intersection of its diagonals as an origin of the coordinate system as shown in figure (7), the meridional was drawn joining the centers of the circles enveloped by the upper and lower airfoil surfaces line segments, starting from the leading edge and ending by the trailing edge of the airfoil.

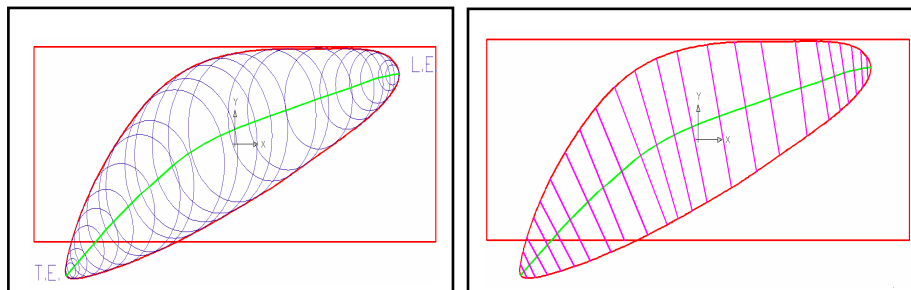


**Fig. 7.** Meridional and normal thickness at 25% radius station.

Coordinates of meridional points and normal thickness were measured in Cartesian (x,y,z,t) coordinates and then transformed into cylindrical (r,θ,z,t) coordinates.

#### Creating and Running an RθZT File for the Propeller Blade Data

An RθZT was created and imported to CFX blade Gen., this file contains the propeller geometric data (the number of blades, number of layers in which each layer is placed at specified span ratio measured from the hub to the tip of the propeller, cylindrical coordinates in addition to normal thickness of points of each layer as shown in Fig. 8.

2(number of blades)	0(number of splitters)	N(normal thickness flag)	
0.0(pitch fraction)	7(number of layers)	63(number of points)	
0.000000000(Span ratio of the first layer)			
R	$\theta$	Z	T
120.000000	0.366503000	-100.000000	0.000000000
120.000000	0.366503000	-22.3505000	6.98426000
120.000000	0.350474379	-21.5453783	8.87957922
120.000000	0.333844476	-20.7402567	11.3091070
120.000000	0.316678670	-19.9351350	12.9937093
120.000000	0.299040451	-19.1300133	14.4917938
.....	.....	.....	.....
<b>0.244411741 81</b>	.....	.....	.....
.....	.....	.....	.....
<b>0.367618010 81</b>	.....	.....	.....
.....	.....	.....	.....
<b>0.631196204 81</b>	.....	.....	.....
.....	.....	.....	.....
<b>0.758722663 81</b>	.....	.....	.....
.....	.....	.....	.....
<b>0.950174517 81</b>	.....	.....	.....
.....	.....	.....	.....
<b>1.00000000 63</b>	.....	.....	.....
.....	.....	.....	.....

**Fig. 8.** R $\theta$ ZT file.

Running the R $\theta$ ZT file in CFX Blade Generator created a 3D CAD model for the propeller blade by generating the surfaces between the layers defined in the R $\theta$ ZT file, the 3D CAD model can be transported to other CAD software with different file formats like IGES or DXF as shown in Fig. 9.

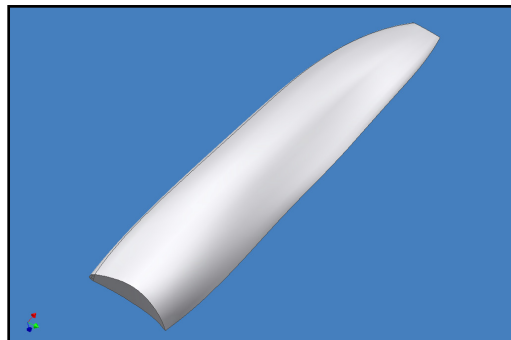


**Fig. 9.** An IGES 3D Solid model of the propeller blade.

The software has the capability of creating graphical representation for the relations between main geometrical parameters, Fig.10 represents the normal thickness along the meridional at recommended radii stations.

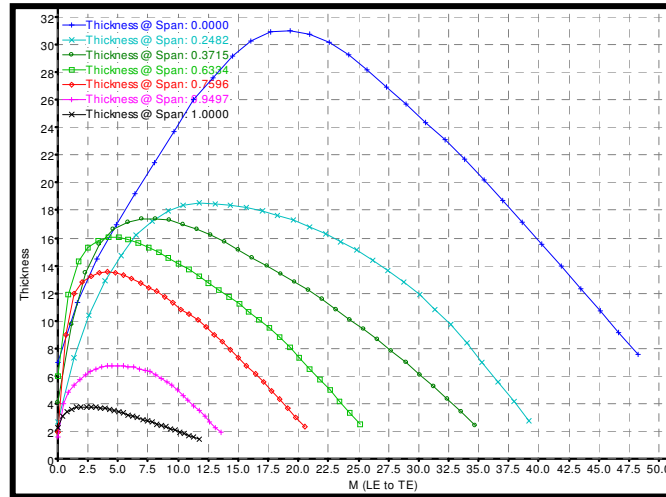


**Fig.10.** Normal thickness vs the meridional.

### CFD Solution of the Propeller using CFX Blade Gen. +

A CFD model for the propeller was built using the CAD model created by CFX blade Gen., and solved numerically in order to confirm and validate the geometry measured by the 3D Laser scanner before manufacture a prototype. The solution was implemented using CFX blade Gen+.

The numerical solution of the Navier–Stokes equations for turbulent flow is extremely difficult, attempts to solve turbulent flow using a laminar solver typically result in a time-unsteady solution, which fails to converge appropriately.

$$\rho \left( \frac{\partial \mathbf{v}}{\partial t} + \mathbf{v} \cdot \nabla \mathbf{v} \right) = -\nabla p + \nabla \cdot \mathbf{T} + \mathbf{f}$$

In studying turbulent flows, the objective is to obtain a theory or a model that can yield quantities of interest, such as velocities. The chief difficulty in modeling turbulent flow comes from the wide range of length and time scales associated with turbulent flow, and that the governing equations of fluid dynamics contain a non-linear convection term and a non-linear and non-local pressure gradient term.

To counter this, time-averaged equations, the Reynolds-averaged Navier–Stokes equations (RANS), supplemented with turbulence model Spalart-Allmaras model is used in CFX solution. The governing equations are solved over discrete control volumes. Finite volume methods recast the governing partial differential equations (typically the Navier-Stokes equations) in a conservative form, and then discretize the new equation. This guarantees the conservation of fluxes through a particular control volume. The finite volume equation yields governing equations in the form,

$$\frac{\partial}{\partial t} \iiint Q dV + \iint F d\mathbf{A} = 0,$$

where  $Q$  is the vector of conserved variables,  $F$  is the vector of fluxes,  $V$  is the volume of the control volume element, and  $A$  is the surface area of the control volume element.

## Solution Procedure

### Grid generation

The normal Grid refinement level was chosen with grid refinement factor 1 and grid inflation layers 3, the number of nodes were found to be 20672.

### Fluid model

Calculating the value of the tip speed, the tip was found to be out of compressibility effects, so it was decided to use the incompressible flow type and a turbulent viscosity model. A Spalart-Allmaras turbulence model was used by the software.

### Boundary and Initial Conditions

To the run specification the mass flow exit choice was selected for incompressible flow (recommended by software manual), it was estimated to be 15.4 kg/sec and the operating conditions for the device were set as follows in Table 1.

**Table 1.** Solution convergence summary.

Rotation rate:	3000 rpm
Inlet swirl angle:	0 degree
Inlet total pressure:	101325 Pa
Inlet total temperature:	300 K

### Solution convergence

The target Residual was set to be 5e-5, the maximum number of iterations of was set to be 200 iterations and for the time step scaling the Auto compute option was chosen as it provides a robust, conservative time step and convergence rate.

The solution convergence plots are shown in Fig. 16. For RMS residuals, mass flow imbalance (Delta M) between inlet and outlet, change in total adiabatic efficiency (Effic.) between inlet and outlet and head rise between inlet and outlet.

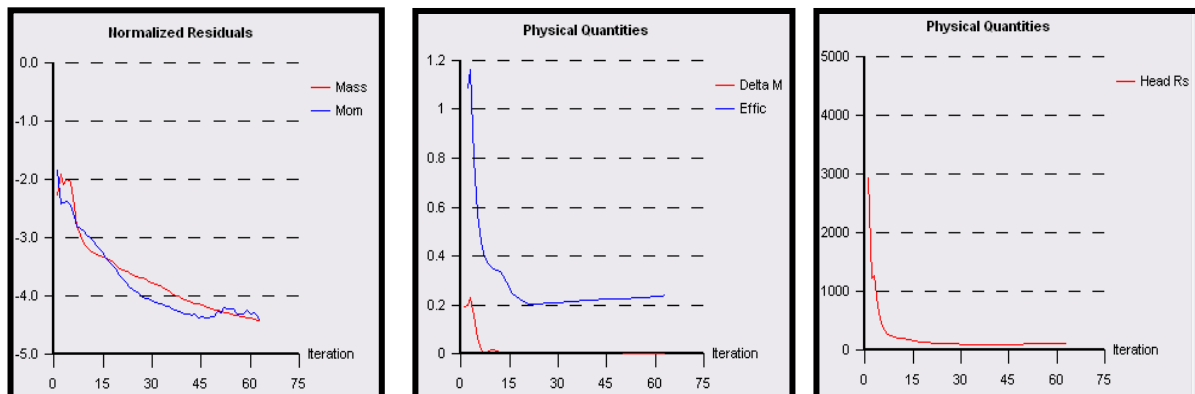


**Fig. 16.** Convergence Plots.

The solution reached the target residual and all RMS residual and global imbalances were below their target criteria as shown in the summary below.

**Table 2.** Solution convergence summary.

Number Iterations	63
Mass Residual	3.7e-005
Momentum Residual	3.8e-005
Energy Residual	0.0e+000
Inlet Mass Flow	7.7022e+000 kg/s
Outlet Mass Flow	-7.7020e+000 kg/s
Mass Imbalance	0.0026 %
Momentum Imbalance	-0.0861 %

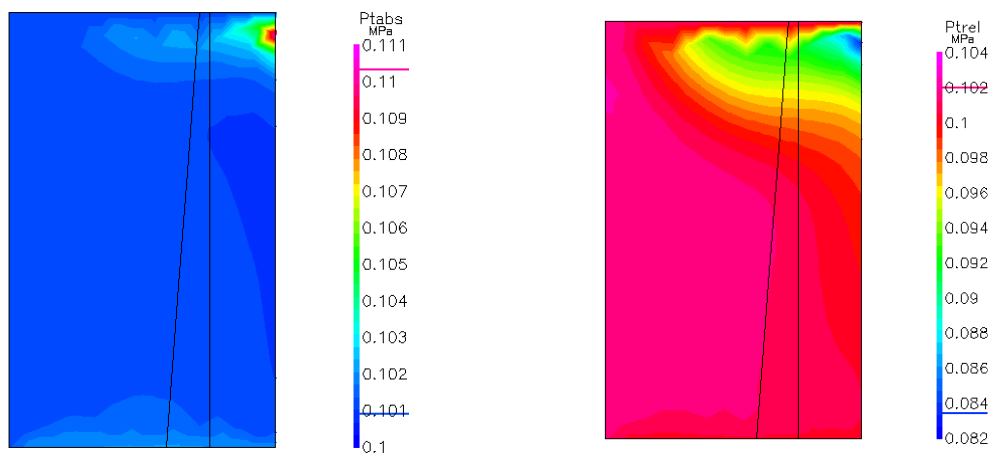
### Solution Results

The program customized report for the results contains the following results:

#### Direct plots

##### Meridional plots

Figure (17)a represents the meridional contour plot of the total absolute pressure while Fig. (17)b shows the relative total pressure contour plot where the effect of the propeller blade appears on the flow.

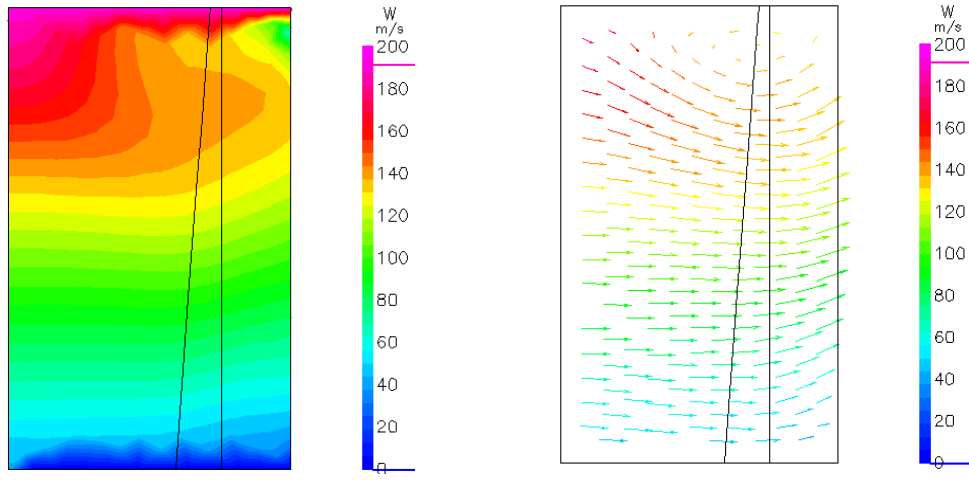


a. Contour of  $P_{tabs}$  at 0% Meridional

b. Contour of  $P_{rel}$  at 0 % Meridional

**Fig.17.** Meridional pressure contour plot.

Figure (18)a and Fig. (18)b represent contour and vector plots of the relative total velocity respectively, the velocity increases as the radius increases due to the increase of the tangential velocity component across the blade radius.



a. Contour of W at 0 % Meridional      b. Vector Plot of W at 0% Merid

**Fig.18.** Meridional velocity contour and vector plots.

### Span-Wise plots

Figure (19) shows the blade loading i.e. the pressure distribution over the pressure and suction surfaces of the airfoil at 75% radius station which is taken as a reference section for the blade.

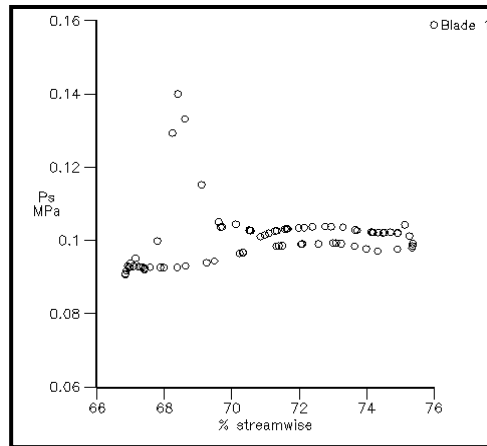
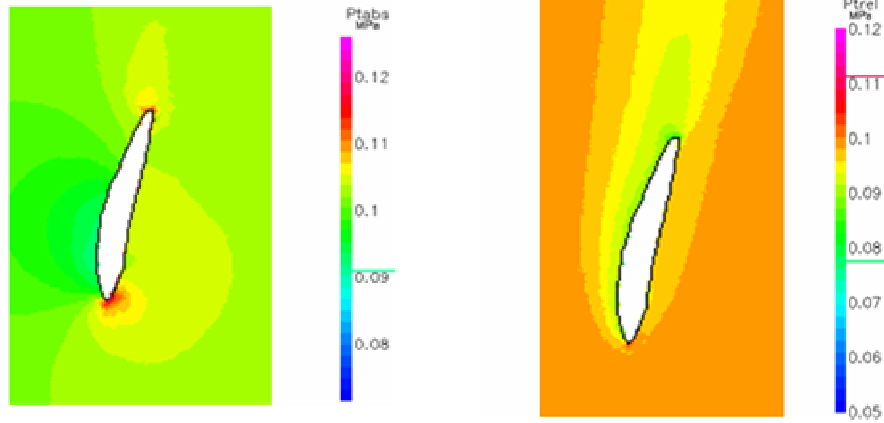


**Fig.19.** Blade loading at 75% span.

Figures (20)a and (20)b shows the contour plot of the absolute and relative total pressure around the 75% radius station airfoil. The change in the colors shows the pressure difference between the pressure and suction sides of the airfoil.

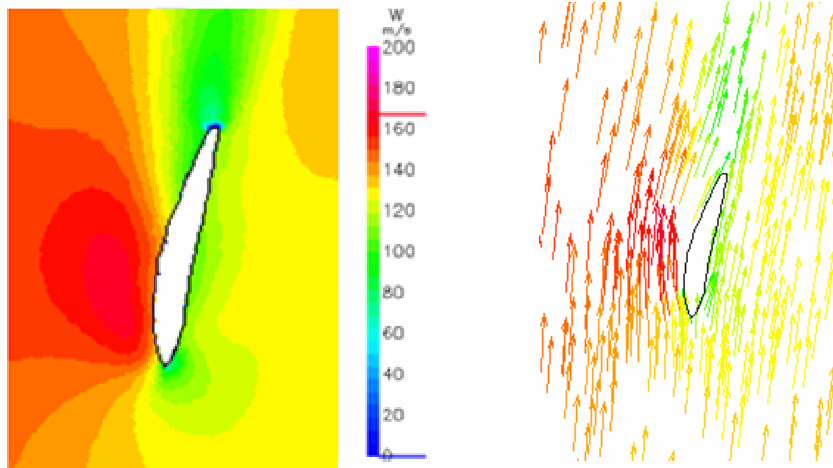
Figures (21)a and (21)b show the contour and vector plots of the total relative velocity around the 75% radius station, respectively.

The span wise distribution of the flow deviation angle ( $\delta$ ) is shown in figure (22)a the value increases in the negative direction due to the blade twist increase from the root to the tip. And the same behavior appears for the same reason in figure (22)b that shows the flow incidence angle ( $I$ ) span wise distribution.



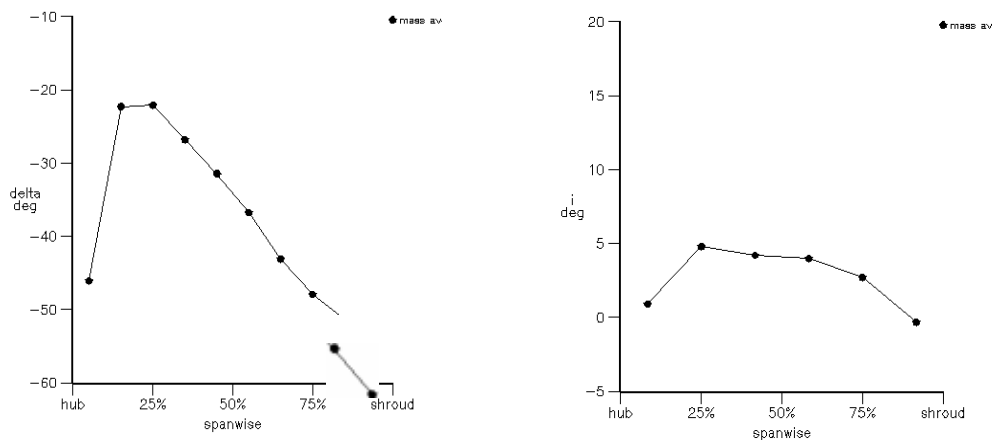
a. Contour of absolute pressure at 75% Span      b. Contour of relative pressure at 75% Span

**Fig. 20.** Pressure contours at 75% radius station.



a. Contour of W at 75% Span      b. Vector Plot of W at 75% Span

**Fig. 21.** Total relative velocity contour and vector plots.

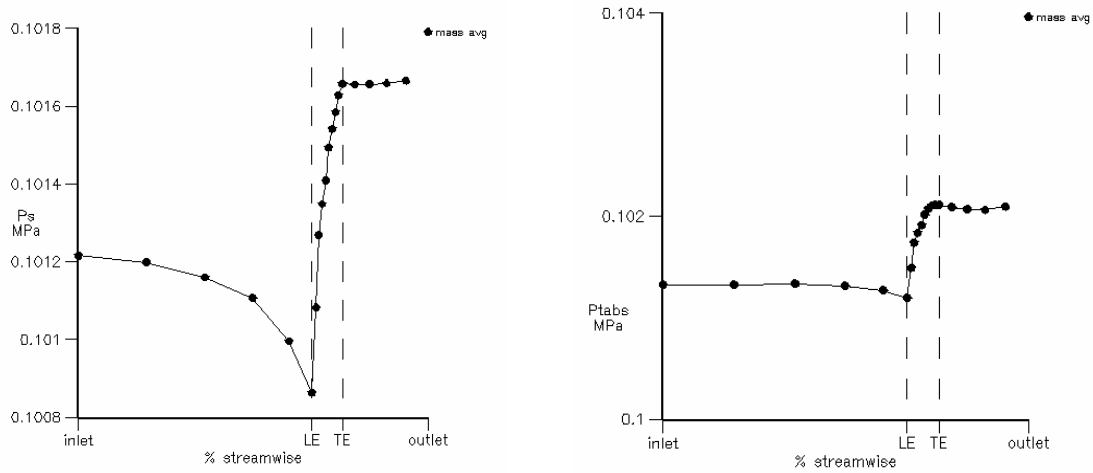


a. Span wise Plot of delta at Blade TE      b. Span wise Plot of i at Blade LE

**Fig.22.** Flow angles span wise distribution.

**Stream-Wise plots**

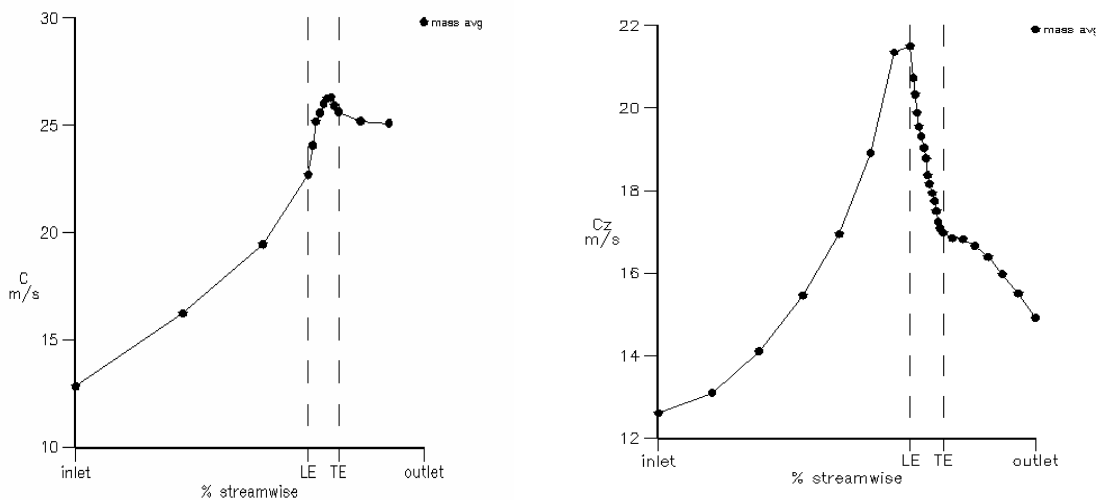
The stream-wise plots of the static and total absolute pressure are shown in figures (23)a and (23)b, respectively. The pressure increases from the leading edge to the trailing edge, reaching its maximum values just down stream the blade and starts to decrease again down stream due to the vanishing of the propeller effect.



a. Stream wise Plot of static pressure      b. Stream wise Plot of absolute pressure

**Fig. 23.** Pressure stream wise plot.

The absolute total velocity plot in figure (24)a shows that the propeller has raised the flow velocity from the static condition at zero velocity to a maximum value of 26 m/sec down stream the blade before the velocity drops again when the propeller effect vanishes. And from figure (24)b the axial velocity component reaches 17 m/sec just down stream the propeller blade which was 15.5 m/sec in the slicing method.



a. Stream wise Plot of total velocity      b. Stream wise Plot of Cz

**Fig.24.** Velocity stream wise plots.

## Calculated Results

The calculation results for the inlet, outlet and total flow properties are shown in tables (1) and (2) as follows:

**Table 3.** Inlet and outlet flow properties.

Flow Properties	Inlet	Outlet
Mass flow In	15.508 kg/sec	15.4236 kg/sec
P Total In	101318 Pa	102143 Pa
T Total In	300.087 K	300.38 k
Inlet flow angle abs	-6.51673°	50.3178 °

**Table 4.** Total Computed Results.

Mass Flow Rate	15.408 kg/s
Volume Flow Rate	13.0025 m <sup>3</sup> /s
Total Blade Torque	52.4519 N-m
Total Efficiency (LE-TE)	0.701546
Static Efficiency (LE-TE)	0.590071
Thrust	267 N

The results of the CFD solution of the propeller model resulted in a value for the total thrust which was 267 Newton and this equal to 60 Pound force. This value of thrust was very close to the propeller specifications mention in its catalogue data [7].

## CONCLUSION

Computation simulation now stands as an equal partner with mathematical analysis and experimental inquiry. CFD has become an effective tool to uncover fluid phenomena and goals more rapidly and cost effectively.

CFD analysis has succeeded to validate the measured geometry, as the CFD results of the propeller thrust was very close to the available thrust data.

Despite of conventional propeller measuring methods which are inaccurate and destructive like the slicing method, new measuring method based on laser scanning technology can be reliable in reverse engineering purposes like measuring complex shapes as propellers.

The Laser scanning technology is a very successful method in measuring, and exporting measured geometric data for complex scanned surfaces like propellers with high accuracy, reliable, robust and nondestructive manner. This has given a great assistance in manufacturing prototypes for the scanned data.

Building a 3D CAD model for a turbo machine blade must be done using special blade generation software instead of using general case CAD modelers.

## REFERENCES

- [1] Alex Varv, “Hand Crafted Propellers Handbook”, McGraw-Hill, 1967.
- [2] HydroComp Inc., “Practical Propeller Modeling: From Concept to 3D CAD”. Report No. 131, Durham, NH 03824 USA, May 2001.
- [3] Chin-Yeh Hsin, Shean-Kwang Chou and Wei-Chung Chen “A New Propeller Design Method for POD Propulsion System”, National Taiwan Ocean University, 2002.
- [4] W. A. Wahba, “Design Optimization of Centrifugal Impellers using Parallel Genetic Algorithm”, School of Mechanical Engineering, Cranfield university, 1999.
- [5] A. Elnashar, W. Wahba and M. Abdurrahman “Three Dimensional Multi Objective Design Optimization Of Centrifugal Compressor Impeller”, 12-th ASAT Conference, 29-31 May 2007.
- [6] Glauert H. “The Elements of Aerofoil and Airscrew Theory”, University Press, Cambridge, 1959.
- [7] The Powered Para-glider Catalogue.